Eur Biophys J (2007) 36:805–813
DOI 10.1007/s00249-007-0151-5

ORIGINAL PAPER

Thermal stability effects of removing the type-2 copper ligand His306 at the interface of nitrite reductase subunits

Andrea Stirpe · Luigi Sportelli · Hein Wijma · Martin Ph. Verbeet · Rita Guzzi

Received: 22 December 2006 / Revised: 22 February 2007 / Accepted: 26 February 2007 / Published online: 16 March 2007

Abstract Nitrite reductase (NiR) is a highly stable trimeric protein, which denatures via an intermediate, $N_3 \overset{k}{\leftrightarrow} U_3 \overset{k}{\rightarrow} F$ (N—native, U—unfolded and F—final). To understand the role of interfacial residues on protein stability, a type-2 copper site ligand, His306, has been mutated to an alanine. The characterization of the native state of the mutated protein highlights that this mutation prevents copper ions from binding to the type-2 site and eliminates catalytic activity. No significant alteration of the geometry of the type-1 site is observed. Study of the thermal denaturation of this His306Ala NiR variant by differential scanning calorimetry shows an endothermic irreversible profile, with maximum heat absorption at $T_{max} \approx 85°C$, i.e., 15°C lower than the corresponding value found for wild-type protein. The reduction of the protein thermal stability induced by the His306Ala replacement was also shown by optical spectroscopy. The denaturation pathway of the variant is compatible with the kinetic model $N_3 \overset{k}{\rightarrow} F_3$, where the protein irreversibly passes from the native to the final state. No evidence of subunits' dissociation has been found within the unfolding process. The results show that the type-2 copper sites, situated at the interface of two monomers, significantly contribute to both the stability and the denaturation mechanism of NiR.

A. Stirpe · L. Sportelli · R. Guzzi (✉)
Dipartimento di Fisica e Unità CNISM,
Università della Calabria, Ponte P. Bucci, Cubo 31C,
87036 Arcavacata di Rende, Cosenza, Italy
e-mail: guzzi@fis.unical.it

H. Wijma · M. Ph.Verbeet
Gorleaus Laboratories, Metallo Protein Group,
Leiden University, P.O. Box 9502,
2300 RA Leiden, The Netherlands

Keywords Nitrite reductase mutant · Thermal stability · Type-2 copper · Two-state irreversible model

Introduction

Approximately one third of all proteins fold in structures consisting of more than one subunit. Most of these oligomeric proteins are homo-oligomers with internal symmetry. Reasons why large proteins are naturally favored over smaller ones include folding efficiency, stability against denaturation, as well as functional advantages (Goodsell and Olson 2000; Ali and Imperiali 2005). Subunit interactions of oligomeric proteins, mainly of hydrophobic character, play an important role in the stability, assembly and function of proteins. A suitable strategy to study the interface interactions and their contribution to the protein stability is to perform specific mutations within this region. However, there are few examples in literature of folding studies on oligomeric proteins in both wild-type (wt) and mutated form. Mutations within the dimeric interface for *Plasmodium falciparum* triosephosphate isomerase have resulted in the formation of monomeric and dimeric species in dynamic equilibrium together with a reduced stability (Maithal et al. 2002). Such a reduced stability has also been observed in superoxide dismutase (Ramilo et al. 1999; Edwards et al. 2001).

Nitrite reductase (NiR) from *Alcaligenes faecalis* S-6 is a homotrimeric copper-containing protein, which catalyzes the reduction of nitrite to nitric oxide.

It is a symmetric protein (Fig. 1a) in which each monomer is subdivided in two domains (shown in Fig. 1a as blue and silver) with a β-barrel secondary structure (Murphy et al. 1995, 1997; Adman et al. 1995) and contains one type-1 Cu and one type-2 Cu. In the type-1 site,

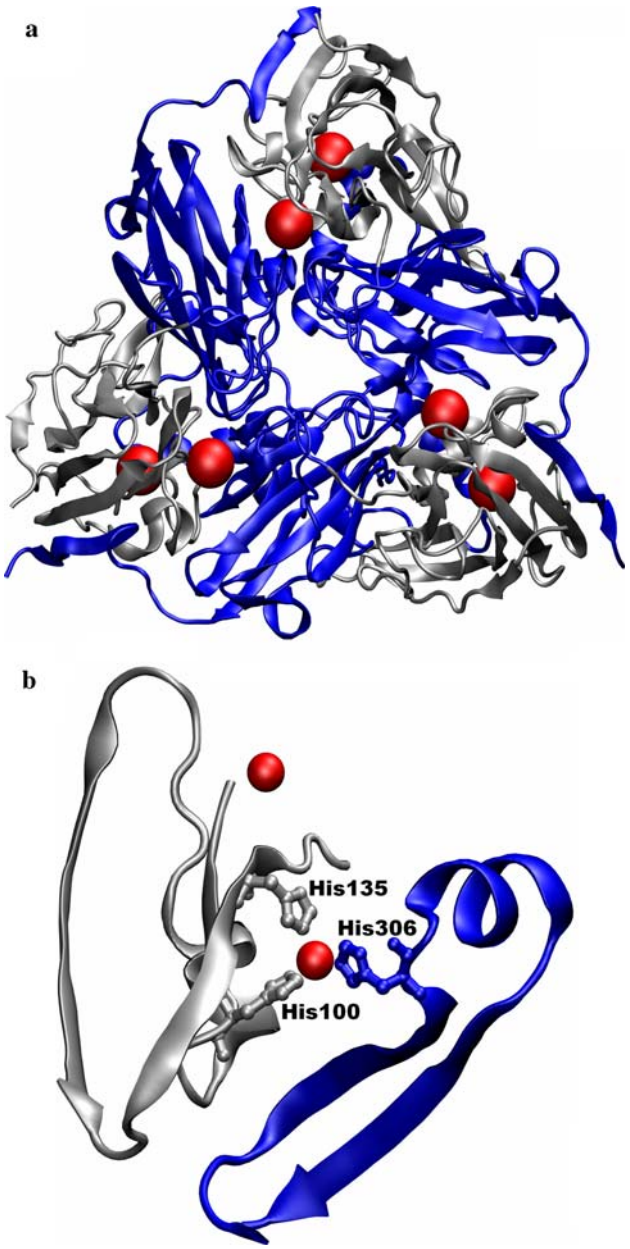

Fig. 1 **a** Crystal structure of wild type NiR. The two subunits of each monomer are drawn in *blue* and *silver*. The six copper atoms are represented by *red spheres*. **b** The site of mutation: the type-2 copper, His135 and His100 from one subunit and His306A from the adjacent subunit

the copper ion is coordinated by His95, Cys136, His145 and Met150 in a coordination typical of the monomeric cupredoxins, with histidine and cysteine residues arranged in a distorted trigonal-planar geometry, and the methionine as a weaker axial ligand. The type-2 site is located at the interface between two monomers and is bound by a water molecule and three histidines residues; His100 and His135 from one subunit and His306 from the adjacent subunit (Fig. 1b). His306 is hydrogen bonded to the main-chain carbonyl of Ala248, whereas His100 and the solvent molecule coordinated to the copper ion form hydrogen bonds with the two carboxylate groups in the second coordination sphere of the copper ion: Glu278 and Asp98, respectively (Murphy et al. 1995; Kallrot et al. 2005). Crystallographic studies (Godden et al. 1991; Murphy et al. 1997) have indicated that the type-2 site is the site at which nitrite binds. The specific activity of the protein correlates with the amount of copper at the type-2 site (Libby and Averill 1992). The two sites are only 12.5 Å far apart and covalently connected through the Cys136 (type-1 Cu ligand) and His135 (type-2 Cu ligand) residues.

In this investigation the NiR variant in which the histidine 306 was replaced by an alanine residue (H306A NiR) has been created with the aim to investigate the role of a mutation within the intersubunit region on the thermal stability of NiR. In addition, the mutated residue also coordinates the type-2 copper ion. Thermodynamic analysis of protein samples in solution has been performed by using calorimetric and spectroscopic techniques. Differential scanning calorimetry (DSC) is a powerful approach, which provides information on the energetics of the transition between the native and the denaturated states. Moreover, the presence of copper centers with optical and magnetic properties allows monitoring the thermal induced conformational changes in their microenvironments.

The results obtained on H306A NiR show that the mutation does not affect the global folding of the protein although it prevents the binding of the copper ion in the catalytic sites. The stability of the NiR mutant is significantly reduced compared to that of the wild-type protein (Stirpe et al. 2005) suggesting that histidine 306 has both a structural and functional role.

Materials and methods

Protein purification, copper content and catalytic activity

For expression and mutagenesis, a pET28b-based vector (Boulanger et al. 2000) containing NiR gene from *A. faecalis* S-6 (Nishiyama et al. 1993) was used. For introduction of the mutations the following primers were used together with standard DNA techniques; H306A forward primer, CAT CTA CGC CTA TGT GAA C**GC** **C**AA TCT GAT CGA **A**GC TTT TGA ACT CGG CGC TGC; H306A reverse primer, GCA GCG CCG AGT TCA AAA GC**T** TCG ATC AGA TT**G** **GC**G TTC ACA TAG GCG TAG ATG (*HindIII* restriction site that was introduced by a silent mutation is shown in italics; The altered bases are shown in bold). Expression and purification of NiR were achieved as described previously (Wijma et al. 2003). The

Cu-content was determined with bicinchoninic acid (Brenner and Harris 1995). Activity assays with reduced pseudoazurin as the electron donor were done in 50 mM MES buffer, pH 6.0. For the calorimetric and spectroscopic measurements, the samples were prepared in 20 mM MOPS buffer, pH = 7.0.

Differential scanning calorimetry

Calorimetric experiments on H306A NiR samples were performed with a VP-DSC MicroCalorimeter (MicroCal, Inc.), with cell volumes of 0.52 ml. The temperature resolution is ±0.1°C. The samples were degassed before measurements: they were scanned from 20 to 120°C at different scan rates (15, 30, 60 and 90°C h^{-1}). The protein concentration was 27 μM, except when otherwise indicated. To obtain a reproducible baseline, at least four buffers versus buffer scans were performed. After the reference measurements, the sample cell was emptied, reloaded with the protein solution and equilibrated for 50 min at 20°C. The irreversibility of the transition was verified by performing several scans in which the final temperature varied from above the temperature of maximum heat absorption (T_{max}) to the end of the endothermic thermal transition. Then the sample was cooled to 20°C and a second scan in the 20–120°C temperature range was carried out. The data were analyzed by using Origin software (MicroCal). All the $C_{p_{exc}}$ curves were obtained from the calorimetric profiles baseline corrected and concentration normalized. The simulation of the experimental DSC thermograms was performed by using an in-house program in MatLab environment. The accuracy of simulation has been verified by the m value (kJ mol^{-1} K^{-1}), as previously described (Stirpe et al. 2005).

Spectroscopy

Optically monitored melting thermograms were carried out with a JASCO 7850 spectrophotometer equipped with a Peltier thermostatted cell, model TPU-436 (precision ± 0.5°C), and an EHC-441 temperature programmer. Quartz cuvettes with a 1-cm optical path were used throughout. Absorbance at a fixed wavelength (λ = 460 nm) was followed over a temperature range from 20 to 95°C, at the same scan rates of the DSC measurements. Protein concentrations amounted to 25 μM. At the end of each experiment, the temperature was lowered to 20°C and then an optical spectrum was recorded to check for refolding.

The EPR experiments were carried out with a Bruker ESP 300 X band spectrometer, equipped with the ESP 1600 data acquisition system. The experimental conditions were as follows: 100 kHz magnetic field modulation, 10 mW microwave power and 5 Gauss peak-to-peak magnetic field modulation amplitude. All EPR spectra were recorded at –196°C; as regards the temperature dependence studies, the protein samples were incubated for 10 min at different temperatures (according to the calorimetric data) and then rapidly plunged into a finger dewar containing liquid nitrogen.

Results and discussion

The native state of H306A NiR

In Fig. 2a are reported the UV-Vis spectra of wild type (line a) and H306A NiR (line b). Both forms of NiR show the following similar optical features: three bands with absorption maximum at 390, 460 and 590 nm, assigned to ligand–metal charge transfer transitions from S(Met) (the

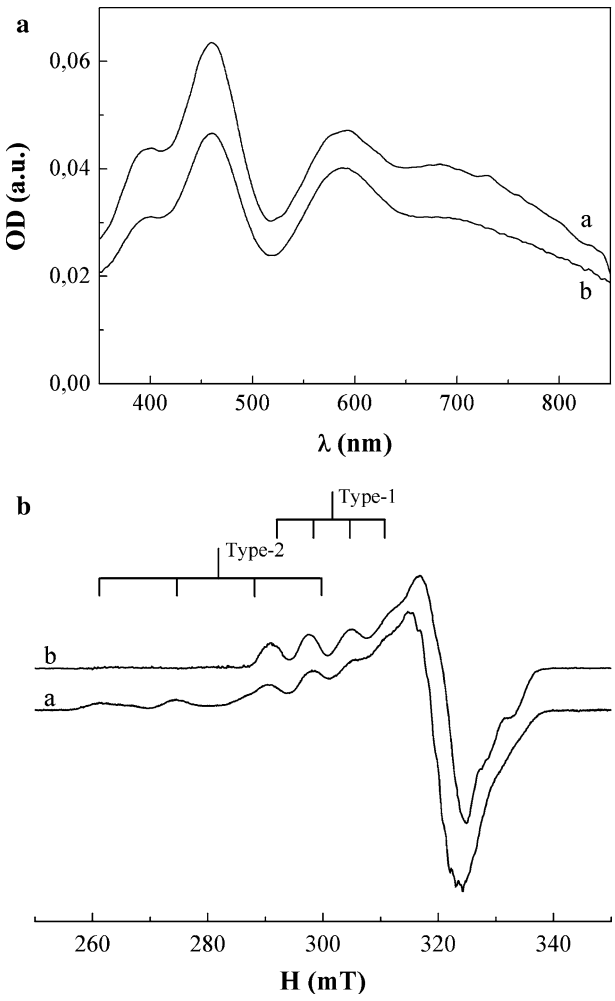

Fig. 2 **a** UV-Vis spectra of H306A NiR (*line b*) and wt NiR (*line a*) recorded at room temperature. **b** Comparison of the EPR spectra of H306A NiR (*line b*) and wt NiR (*line a*), recorded at –196°C

first band) and S(Cys) (the other two bands) to Cu (II) ion (LaCroix et al. 1996). Additionally, a broad band in the 700–810 nm wavelength range, which originates from d → d transitions of the type-1 (LaCroix et al. 1996) and only for an insignificant part from the type-2 coppers (Wijma et al. 2003), can be noted. The similarity of the absorption spectra suggests that the geometry of the type-1 copper sites is not strongly influenced by the nearby mutation in the type-2 copper site. This result is quite different from that found for the H129V mutant of *Alcaligenes xylosoxidans* NiR (AxNiR), where a mutation of a type-2 copper ligand induces a big effect on the geometry of the type-1 site (Ellis et al. 2004). Both the optical and EPR spectra show a significant alteration with respect to the wild-type protein.

In Fig. 2b the EPR spectra at –196°C of the wild type (line a) and H306A mutated NiR (line b) are compared. The typical features of both type-1 and type-2 copper sites are observed in the wild-type protein. In contrast, in the H306A variant of the protein, the type-2 EPR signal is completely missing. Copper content analysis on the mutated protein reveals that one copper atom per monomer is found (1.0–1.2 Cu atoms per monomer). Furthermore, the 2,000-fold lower than wt catalytic activity (turn-over rate 0.43 s^{-1}) for a batch with 1.2 Cu atoms per monomer is in agreement with the His306 being essential for the formation of a functional catalytic site in NiR.

Numerous are the type-1 copper ligand NiR variants appeared in literature (Murphy et al. 1995; Wijma et al. 2003; Hough et al. 2005). In these cases, the copper ion is almost always present in the type-1 site, but the redox potential and the catalytic activity are strongly modified, reduced or in some cases absent as for the C130A AxNiR mutant. In this mutant, the copper ion is missing in the type-1 site but a small amount (about 15%) of copper was found in the type-2 site (Hough et al. 2005).

Instead, as concerns the type-2 copper mutants the earlier-mentioned H129V AxNiR mutant, is the only type-2 ligand NiR mutant investigated so far (Ellis et al. 2004). In contrast to our result, in this mutant the copper ion is still bound to the type-2 site in a novel bis–His Cu site coordination and affects also the geometry of the type-1 copper site.

The EPR spectrum of the wt NiR in Fig. 2b clearly shows in the high field region a super-hyperfine structure, which is no longer resolved in the mutant. Therefore, this structure is probably due to the interaction of the unpaired electron spin of the $3d_{x^2-y^2}$ Cu (II) ion with the nuclear spin of the ligand nitrogen atoms (McGarvey 1967) of the type-2 copper.

The optical and magnetic spectra here observed for H306A NiR show similar features to those found for the type-2 Cu-depleted NiR from *Achromobacter cycloclastes*, which like the *A. faecalis*, belongs to the same spectroscopic class of NiR (Suzuki et al. 1997).

The EPR parameters of type-1 copper sites of native state NiR (Table 1) are slightly different from those of the corresponding ion in the wild-type protein (see Table 3, in Stirpe et al. 2005). In particular, a slight increase in the $A_{\parallel}$ hyperfine splitting constant from 7.15 to 7.41 mT can be observed. Such a variation, which is presumably due to the absence of overlapping between the two types of copper in the mutant, has also been found in laccase from *Coriolus hirsutus* (Koroleva et al. 2001).

Calorimetric analysis of the thermal stability of H306A NiR

Figure 3a shows the calorimetric curve of H306A NiR (solid line), in 20 mM MOPS buffer, pH 7.0, recorded at the scan rate of 60°C h^{-1}, in the 20–120°C temperature range. The DSC profile displays a sharp, endothermic peak with maximum heat absorption at T_{max} = 84.7°C, i.e., 15°C lower than that shown by the wt protein (dashed line) (Stirpe et al. 2005). The thermal transition occurs on a short temperature range (≈15°C), indicating a high transition cooperativity.

The second scan of the previously scanned sample did not show any heat absorption, so that the thermal unfolding of H306A NiR mutant is still irreversible just like that of the wt protein and it cannot be analyzed in terms of equilibrium thermodynamics. Protein aggregation, deamination of asparagine and/or glutamine residues, loss of cofactors as well as the presence of dissolved molecular oxygen in solution and its reaction with cysteines forming disulfides and sulfenic acid can be responsible for the irreversibility of the thermal denaturation (Zale and Klibanov 1986; Sandberg et al. 2002; Jacob et al. 2004; Tigerstrom et al. 2004).

The DSC profiles are also scan rate dependent as can be seen from Fig. 4, where the $C_{p_{exc}}$ transition curves of H306A mutant recorded at 15, 30, 60 and 90°C h^{-1} are

Table 1 The $g_{\parallel}$ and $A_{\parallel}$ values determined by the experimental EPR spectra recorded at –196°C for H306A, after a pre-heating treatment as indicated in the methods section

Temperature (°C)	Type-1		Type-2	
	$g_{\parallel}$	$A_{\parallel}$ mT^{-1}	$g_{\parallel}$	$A_{\parallel}$ mT^{-1}
Native state	2.1946	7.41	/	/
50.0	2.1935	7.47	/	/
77.0	2.1892	7.67	/	/
84.5	/	/	2.4182	17.13
92.0	/	/	2.4153	17.31
100.0	/	/	2.4163	16.56

The uncertainties in $g_{\parallel}$ and $A_{\parallel}$ values are ±0.0002 and ±0.02 mT, respectively

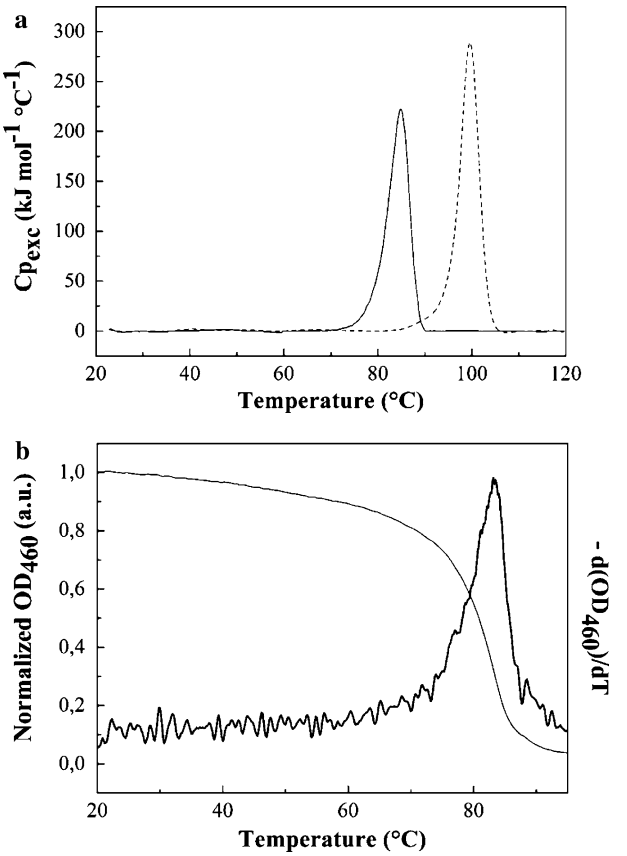

Fig. 3 **a** Differential scanning calorimetry profile of H306A NiR in MOPS 20 mM (pH = 7.0), recorded at the scan rate of 60°C h^{-1} (*solid line*). The protein concentration is 27 μM. *Dashed line* is the DSC thermogram of the wild type protein. **b** Normalized OD_{460} (*thin line*) and first derivative spectrum, multiplied by –1, of the optical thermogram (*thick line*) vs. temperature of H306A NiR, recorded at the same scan rate of the calorimetric profile

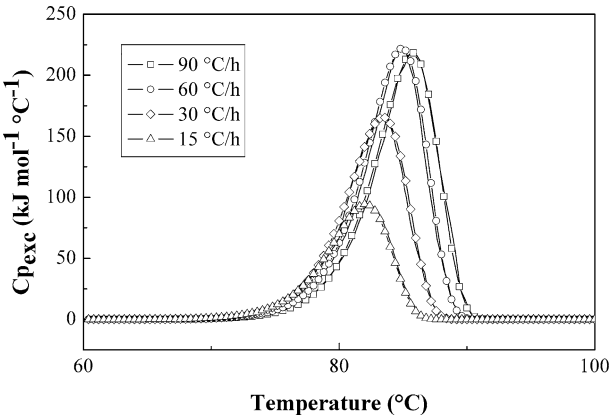

Fig. 4 Comparison of experimental (*solid lines*) and simulated transition curves (*dashed* + *symbol lines*) at different scan rates. Equation 2 was used for the simulation of the experimental curves. The optimized parameters are reported in Table 3

Table 2 Scanning rate dependence of the optical transition temperature, T_t, the maximum heat absorption temperature, T_{max}, and the experimental denaturation enthalpy, ΔH_{cal}, for H306A NiR

Scan rate (°C h^{-1})	Optical density [T_t (°C)]	Differential scanning calorimetry	
		T_{max} (°C)	$\Delta H_{cal} \times 10^2$ (kJ mol^{-1})
15	80.6	82.3	6.2 ± 0.2
30	82.0	83.5	10.1 ± 0.3
60	83.2	84.7	13.3 ± 0.2
90	84.8	85.9	13.9 ± 0.3

Estimated error on T in DSC measurements is ±0.1°C while for OD measurements this is ±0.5°C

ΔH_{cal} is expressed as mean ± standard deviation

shown. In Table 2 the corresponding temperatures of maximum heat absorption, T_{max}, and the calorimetric enthalpies, ΔH_{cal}, are listed. Such parameters strongly depend on the heating rate: by decreasing the velocity, the temperature and calorimetric enthalpy are shifted to lower values. Differences in the values of the denaturation enthalpy measured at varying scanning rates can be ascribed to the different final states reached by the enzyme at the different heating rates. Such a situation is realized, for example, when denaturation is accompanied by the formation of aggregates, whose form depends on the scan rate (Lyubarev et al. 1998). The contribution of the aggregation processes is more effective at the lower scan rates, determining the higher difference in the ΔH_{cal} values. At 60 and 90°C h^{-1} the values are very similar (Table 2). Comparing the ΔH_{cal} values between the wt and H306A NiR, a reduction of the denaturation enthalpy of the mutant can be observed at all the scan rates, confirming the lower stability of the mutant. As an example, at the scan rate of 60°C h^{-1} the $\Delta\Delta H_{cal} = \Delta H_{cal}$ (wt) – ΔH_{cal} (mut) = 300 kJ mol^{-1}.

The temperature and enthalpy variations with the scan rate suggest that the denaturation process of H306A NiR is kinetically controlled. To check the existence of possible intermediate reversible states within the unfolding pathway, several DSC measurements were performed on samples, in which the temperature was stopped at $T \geq T_{max}$. These scans were followed by a second scan on the whole temperature range (20–120°C) to evaluate the reversibility ratio of denaturation, i.e., the protein refolding. In the second scan, the peak at 85°C has disappeared. Consequently, the protein transition from the native to the denaturated state cannot be described by the same unfolding model used for the wt NiR, $N_3 \overset{k}{\leftrightarrow} U_3 \overset{k}{\rightarrow} F$. This model involves two steps: (1) reversible unfolding of the native (N) protein; (2) irreversible alteration of the unfolded (U) protein to yield a final (F) state that is unable to fold back to the native one. In H306A NiR, only the N and F states are significantly populated and the denaturation process can be regarded as a one-step irreversible model $N \overset{k}{\rightarrow} F$

(Sanchez-Ruiz *et al.* 1988). The temperature dependence of the first-order kinetic rate constant, k, is given by the Arrhenius equation:

$$k = A\exp\left(-\frac{E_a}{RT}\right) = \exp\left[-\frac{E_a}{R}\left(\frac{1}{T}-\frac{1}{T*}\right)\right] \quad (1)$$

where E_a is the activation energy, T^* is the temperature at which the rate constant value is $k(T^*) = 1\ \text{min}^{-1}$. The denaturation of oligomeric proteins requires disruption of additional molecular interactions over those of monomeric proteins since the inter- as well as intrasubunit interactions make distinct and different contributions to their overall structure and stability (Alber and Matthews 1987; Agashe and Udgaonkar 1995). If the denaturation process is accompanied by the dissociation in monomers, the excess heat capacity versus temperature profile should depend on protein concentration (Sanchez-Ruiz 1992). DSC experiments at different protein concentration ranging from 27 to 140 μM show no significant change of both the shape and the T_{max} value of the thermal profiles (data not shown); therefore, the DSC transitions were mainly dominated by intramolecular processes. This suggests that the observed heat absorption is connected with the melting of a compact structure without simultaneous dissociation into monomers, as already observed in the wt form (Stirpe et al. 2005) and in other multimeric enzymes (Chen et al. 1999; Thorolfsson et al. 2002).

According to these analyses, the two-state kinetic model describing the protein thermal denaturation pathway can be rewritten as: $N_3 \xrightarrow{k} F_3$. To test the validity of this model, the DSC thermograms at the different scan rates were simulated with the following equation (Freire et al. 1990; Kurganov et al. 1997):

$$C_{p_{exc}} = \frac{1}{v}\Delta H\exp\left[-\frac{E_a}{R}\left(\frac{1}{T}-\frac{1}{T*}\right)\right] \times \exp\left\{-\frac{1}{v}\int_{T_0}^{T}\exp\left[-\frac{E_a}{R}\left(\frac{1}{T}-\frac{1}{T*}\right)\right]dT\right\} \quad (2)$$

where v (°C h^{-1}) stands for the scan rate, ΔH is the denaturation enthalpy, T_0 is the onset temperature.

The starting values of ΔH, E_a and T^* can be experimentally estimated. In particular, ΔH can be evaluated from the area under the experimental calorimetric curves.

The activation energy has been obtained by four different methods using the DSC data, as previously described (Stirpe et al. 2005 and references therein). The values are the following:

1. ln (k) vs. $1/T \rightarrow E_a = 454 \pm 19$ kJ mol^{-1};
2. ln (v/T^2_{max}) vs. $1/T \rightarrow E_a = 496 \pm 40$ kJ mol^{-1};
3. ln [ln[$\Delta H_{cal}/(\Delta H_{cal} - \Delta H)$]] vs. $1/T \rightarrow E_a = 453 \pm 3$ kJ mol^{-1};
4. $E_a = \frac{eRT^2_{max}C_{pexc}(T_{max})}{\Delta H_{cal}} = 464 \pm 5$ kJ mol^{-1}.

The activation energy value averaged on the above results is: $\bar{E}_a = 467 \pm 29$ kJ mol^{-1}. This was the starting value for the simulation. The excellent agreement between the E_a values is a further support to the validity of the one-step irreversible model for the thermal denaturation of H306A NiR (Sanchez-Ruiz et al. 1988; Kurganov et al. 1997; Lyubarev et al. 1998; Banerjee and Kishore 2004). The E_a average value is lower compared with that of the native protein (Stirpe et al. 2005): therefore, the thermal denaturation is still an activated process, although requires lower activation energy.

Finally, T^* can be estimated from the x-axis intercept of the Arrhenius plot for k (method I). For the four heating rates, the T^* values are similar and correspond to 86.9 ± 1.0°C (data not shown).

In Fig. 4 the simulated (lines + symbols) and the experimental (solid lines) thermograms of H306A NiR are compared, whereas the parameters used for the simulations are in Table 3. From the visual inspection of Fig. 4 and from the best fit (m value), it is clear that the one-step kinetic model provides a good description of the thermal denaturation of the mutated NiR. Then, the mutation affects not only the stability of the native protein but also the unfolding pathway.

Spectroscopic analysis of the thermal stability of H306A NiR

The temperature-induced variation of the optical absorption at 460 nm can be used to monitor the local conformational changes occurring in the type-1 copper sites. Figure 3b reports the normalized optical absorption variation at $\lambda = 460$ nm (thin line) of H306A NiR recorded in the 20–95°C temperature range at a scan rate of 60°C h^{-1}. The first derivative of the optical thermogram, multiplied by –1, (thick line) shows a single transition, as in the native protein, that occurs at lower temperature: $T_t = 83.2$°C vs. 95.5°C observed in wt NiR. According to the calorimetric

Table 3 Thermodynamic and kinetic parameters used in the simulations of the heat capacity transition curves at different scan rates

v (°C h^{-1})	ΔH (kJ mol^{-1})	E_a (kJ mol^{-1})	T^* (°C)	m (kJ mol^{-1} K^{-1})
15	595	446	87.3	0.42
30	1,035	454	87.0	0.67
60	1,389	457	86.8	0.90
90	1,396	449	86.7	0.71

result, the optical absorption confirms a diminished stability of the mutant as compared to the wild-type protein. It is reasonable to suppose that the substitution of the His306 affects not only the type-2 copper binding site but also the hydrophobic interaction at the subunits interface. Moreover, the elimination of the hydrogen bond formed by His306 with the main-chain carbonyl of Ala248 should be also considered. The thermodynamic consequence is a reduction of the thermal stability. In literature only few examples on thermal studies of multimeric proteins and of their variants at the subunits interface are reported. One of this is the homotetramer human manganese superoxide dismutase where His30 forms a hydrogen bond across the dimer interface and participates in a hydrogen-bonded network that extends to the active site. The substitution of this residue with an alanine reduces the thermal stability of the protein of about 16°C (Ramilo et al. 1999; Edwards et al. 2001). That result compares well with our finding.

Also, the denaturation of the type-1 copper site is irreversible. A_{460} versus T measurements, at the same heating rate of the DSC experiments, give the T_t values reported in Table 2. The comparison of T_t and T_{max} reveals that the T_t values are 1–2°C lower than T_{max} at each scan rate. This difference suggests that the alterations of the copper coordination environment slightly precede the global protein denaturation. A similar behavior has also been observed for wt protein (Stirpe et al. 2005).

More insight into the coordination geometry of the copper environments in H306A NiR, during the denaturation process, can be gained by low temperature EPR spectroscopy. The experiments have been performed following the procedure described in Sect. ''Materials and methods'' and the results are shown in Fig. 5.

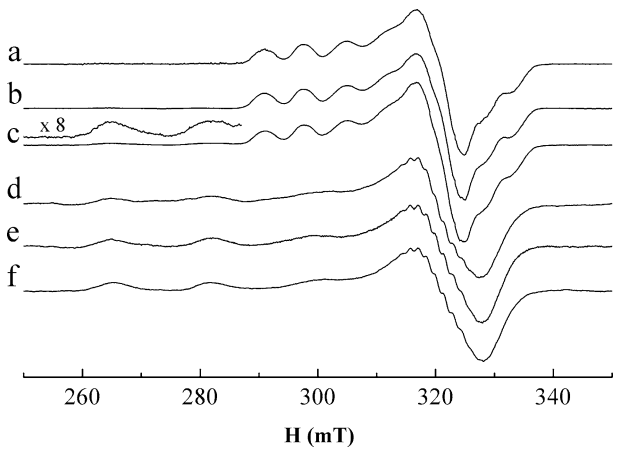

Fig. 5 EPR spectra of H306A NiR from *Alcaligenes faecalis* recorded at –196°C after incubation for 10 min at the following temperatures (°C): (*a*) native state; (*b*) 50.0; (*c*) 77.0; (*d*) 84.5; (*e*) 92.0; (*f*) 100.0

Such a thermal study, also used to investigate the copper centers of laccase (Koroleva et al. 2001), allows to detect only irreversible or slowly reversible structural changes in the copper sites, because the samples are pre-heated to different temperatures for 10 min and the EPR spectra are recorded immediately after freezing.

EPR spectra of H306A NiR do not display significant changes if the protein sample experiences a thermal treatment up to 50°C (lines a, b). Increasing the pre-heating temperature at 77°C (line c), the magnetic signal of H306A NiR still shows the typical type-1 copper features. However, resonance lines of low intensity, in the parallel region of type-2 copper, are also present (as can be observed in the amplification of the low field region). This finding, in agreement with the optical thermogram (Fig. 3b), suggests the beginning of structural changes in the type-1 copper sites. In confirmation of this result, the EPR spectrum recorded after heating of the protein at 85°C (line d) shows a signal exclusively compatible with a type-2 copper; in the high field region a super-hyperfine structure appears. These features persist also after protein samples are pre-heated at higher temperatures (lines e, f). The data obtained indicate a strong effect of the unfolding on the geometry and the coordination atoms of the type-1 copper sites of the mutated protein in the native state. In fact, the copper ligand coordination geometry undergoes a transition from strongly distorted tetrahedral in the native state to square planar in the final state, as suggested by the change of the $A_{\|}$ value from 7.41 to 17.13 mT. Similar conformational transition from the native to the denaturated state is also observed in blue copper proteins (La Rosa et al. 1995; Alcaraz and Donaire 2005; Stirpe et al. 2006). Moreover, the presence of nine super-hyperfine resonance lines indicates that four nitrogen atoms are in the first coordination sphere of the copper of H306A NiR mutant in the denaturated state. This result, also observed in the wt protein, suggests that the two forms of NiR reach the same final state.

Conclusions

The replacement of His306, an interfacial residue belonging to the type-2 copper coordination sphere, with an alanine, affects in a marked way both the thermal stability and the denaturation pathway of NiR. An important consequence of this mutation is that it prevents the binding of the copper ions in the type-2 catalytic site, suggesting that this residue has both a functional and structural role. The modification within the type-2 site weakens the interaction at the interface of the two subunits resulting in a reduced stability of the NiR mutant. The results obtained with DSC, EPR and optical spectroscopy have revealed some common features with the wt protein, i.e., the disruption of the

type-1 copper sites before the transition of the whole protein macromolecule in the denaturated state, the conformational transition from type-1 to type-2 copper at the denaturation temperature and the irreversibility of the thermal transition. The denaturation pathway of the mutated protein is satisfactorily described by a two-state kinetic model, in which the protein irreversibly passes from the native to the final state.

References

Adman ET, Godden JW, Turley S (1995) The structure of copper nitrite-reductase from *Achromobacter cycloclastes* at five pH values, with NO^{-}_{2} bound and with type II copper depleted. J Biol Chem 46:27458–27474

Agashe VR, Udgaonkar JB (1995) Thermodynamics of denaturation of barstar: evidence for cold denaturation and evaluation of the interaction with guanidine hydrochloride. Biochemistry 34:3286–3299

Alber T, Matthews BW (1987) Structure and thermal stability of phage T4 lysozyme. Methods Enzymol 154:511–533

Alcaraz LA, Donaire A (2005) Rapid binding of copper(I) to folded aporusticyanin. FEBS Lett 579:5223–5226

Ali MH, Imperiali B (2005) Protein oligomerization: how and why. Bioorg Med Chem 13:5013–5020

Banerjee T, Kishore N (2004) A differential scanning calorimetric study on the irreversible thermal unfolding of concanavalin A. Thermochim Acta 411:195–201

Boulanger MJ, Kukimoto M, Nishiyama M, Horinouchi S, Murphy MEP (2000) Catalytic roles for two water bridged residues (Asp-98 and His-255) in the active site of copper-containing nitrite reductase. J Biol Chem 275:23957–23964

Brenner AJ, Harris ED (1995) A quantitative test for copper using bicinchoninic acid. Anal Biochem 226:80–84

Chen Y, Mao H, Zhang X, Gong Y, Zhao N (1999) Thermal conformational changes of bovine fibrinogen by differential scanning calorimetry and circular dichroism. Int J Biol Macromol 26:129–134

Edwards RA, Whittaker MM, Whittaker JW, Baker EN, Jameson GB (2001) Removing a hydrogen bond in the dimer interface of *Escherichia coli* manganese superoxide dismutase alters structure and reactivity. Biochemistry 40:4622–4632

Ellis MJ, Antonyuk SV, Strange RW, Sawers G, Eady RR, Hasnain SS (2004) Observation of an unprecedented Cu bis–His site: crystal structure of the H129V mutant of nitrite reductase. Inorg Chem 43:7591–7593

Freire E, van Osdol WW, Mayorga OL, Sanchez-Ruiz JM (1990) Calorimetrically determined dynamics of complex unfolding transitions in proteins. Annu Rev Biophys Biophys Chem 19:159–188

Godden JW, Turley S, Teller DC, Adman ET, Liu MY, Payne WJ, LeGall J (1991) The 2.3 angstrom X-ray structure of nitrite reductase from *Achromobacter cycloclastes*. Science 253:438–442

Goodsell DS, Olson AJ (2000) Structural symmetry and protein function. Annu Rev Biophys Biomol Struct 29:105–153

Hough MA, Ellis MJ, Antonyuk SV, Strange RW, Sawers G, Eady RR, Hasnain SS (2005) High resolution structural studies of mutants provide insights into catalysis and electron transfer processes in copper nitrite reductase. J Mol Biol 350:300–309

Jacob C, Holme AL, Fry FH (2004) The sulfinic acid switch in proteins. Org Biomol Chem 2:1953–1956

Kallrot N, Nilsson K, Rasmussen T, Ryde U (2005) Theoretical study of structure of catalytic of copper site in nitrite reductase. Int J Quantum Chem 102:520–541

Koroleva OV, Stepanova EV, Binukov VI, Timofeev VP, Pfeil W (2001) Temperature-induced changes in copper centers and protein conformation of two fungal laccase from *Coriolus hirsutus* and *Coriolus zonatus*. Biochim Biophys Acta 1547:397–407

Kurganov BI, Lyubarev AE, Sanchez-Ruiz JM, Shnyrov VL (1997) Analysis of differential scanning calorimetry data for proteins. Criteria of validity of one-step mechanism of irreversible protein denaturation. Biophys Chem 69:125–135

LaCroix LB, Shadle SE, Wang Y, Averill BA, Hedman B, Hodgson KO, Solomon EI (1996) Electronic structure of the perturbed blue copper site in nitrite reductase: spectroscopic properties, bonding, and implications for the entatic/rack state. J Am Chem Soc 118:7755–7768

La Rosa C, Grasso DM, Milardi D, Guzzi R, Sportelli L (1995) Thermodynamics of the thermal unfolding of azurin. J Phys Chem 99:14864–14870

Libby E, Averill BA (1992) Evidence that the type 2 copper centers are the site of nitrite reduction by *Achromobacter cycloclastes* nitrite reductase. Biochem Biophys Res Commun 187:1529–1535

Lyubarev AE, Kurganov BI, Burlakova AA, Orlov VN (1998) Irreversible thermal denaturation of uridine phosphorylase from *Escherichia coli* K-12. Biophys Chem 70:247–257

Maithal K, Ravindra G, Nagaraj G, Singh SK, Balaram H, Balaram P (2002) Subunit interface mutation disrupting an aromatic cluster in *Plasmodium falciparum* triosephosphate isomerase: effect on dimer stability. Protein Eng 15:575–584

McGarvey BR (1967) Electron spin resonance of transition metal complexes. In: Carlin R (ed) Transition metal chemistry, vol 3. M. Dekker, New York, pp 90–201

Murphy MEP, Turley S, Kukimoto M, Nishiyama M, Horinouchi S, Sasaki H, Tanokura M, Adman ET (1995) Structure of *Alcaligenes faecalis* nitrite reductase and a copper site mutant, M150E, that contains zinc. Biochemistry 34:12107–12117

Murphy MEP, Turley S, Adman ET (1997) Structure of nitrite bound to copper-containing nitrite reductase from *Alcaligenes faecalis*. J Biol Chem 45:28455–28460

Nishiyama M, Suzuki J, Kukimoto M, Ohnuki T, Horinouchi S, Beppu T (1993) Cloning and characterization of a nitrite reductase gene from *Alcaligenes faecalis* and its expression in *Escherichia coli*. J Gen Microbiol 139:725–733

Ramilo CA, Leveque V, Guan Y, Lepock JR, Tainer JA, Nick HS, Silverman DN (1999) Interrupting the hydrogen bond network at the active site of human manganese superoxide dismutase. J Biol Chem 274:27711–27716

Sanchez-Ruiz JM (1992) Theoretical analysis of Lumry–Eyring models in differential scanning calorimetry. Biophys J 61:921–935

Sanchez-Ruiz JM, Lopez-Lacomba JL, Cortijo M, Mateo PL (1988) Differential scanning calorimetry of the irreversible thermal denaturation of thermolysin. Biochemistry 27:1648–1652

Sandberg A, Leckner J, Shi Y, Schwarz FP, Karlsson BG (2002) Effects of metal ligation and oxygen on the reversibility of the thermal denaturation of *Pseudomonas aeruginosa* azurin. Biochemistry 41:1060–1069

Stirpe A, Guzzi R, Wijma H, Verbeet MPh, Canters GW, Sportelli L (2005) Calorimetric and spectroscopic investigations of the thermal denaturation of wild type nitrite reductase. Biochim Biophys Acta 1752:47–55

Stirpe A, Sportelli L, Guzzi R (2006) A comparative investigation of the thermal unfolding of pseudoazurin in the Cu(II)-holo and apo form. Biopolymers 83:487–497

Suzuki S, Deligeer, Yamaguchi K, Kataoka K, Kobayashi K, Tagawa S, Kohzuma T, Shidara S, Iwasaki H (1997) Spectroscopic characterization and intramolecular electron transfer processes of native and type 2 copper depleted nitrite reductases. J Biol Inor Chem 2:265–274

Thorolfsson M, Ibarra-Molero B, Fojan P, Petersen SB, Sanchez-Ruiz JM, Martinez A (2002) L-phenylalanine binding and domain organization in human phenylalanine hydroxylase: a differential scanning calorimetry study. Biochemistry 41:7573–7585

Tigerstrom A, Schwarz FP, Karlsson BG, Okvist M, Alvarez-Rua C, Maeder D, Robb FT, Sjolin L (2004) Effects of a novel disulfide bond and engineered electrostatic interactions on the thermostability of azurin. Biochemistry 43:12563–12574

Wijma HJ, Boulanger MJ, Molon A, Fittipaldi M, Huber M, Murphy MEP, Verbeet MPh, Canters GW (2003) Reconstitution of the type-1 active site of the H145G/A variants of nitrite reductase by ligand insertion. Biochemistry 42:4075–4083

Zale SE, Klibanov AM (1986) Why does ribonuclease irreversibly inactivate at high temperatures? Biochemistry 25:5432–5444